Development of Theoretical Models for Jet-Induced Effects on V/STOL Aircraft

M.J. Siclari,* D. Migdal,† T.W. Luzzi Jr.,‡
Grumman Aerospace Corporation, Bethpage, N.Y.
J. Barche,§
VFW-Fokker, Bremen, Federal Republic of Germany
and
J.L. Palcza¶
Naval Air Propulsion Test Center, Trenton, N.J.

Successful design and development of V/STOL aircraft requires an understanding and accurate prediction of aircraft forces and moments caused by jet-induced phenomena. Several computerized analytic procedures have been developed using potential flow theoretical solutions to model the entrainment and displacement effects of a propulsion system efflux. The various flow regimes and theoretical models will be described for out-of-ground effect and in-ground effect, where multijet interactions with the ground plane cause significantly increased entrainment and fountain forces. These jet models are coupled with a panel method for calculating the aerodynamic forces and moments. Excellent agreement between calculated and model test data is displayed.

Introduction

THIS paper deals with recently developed prediction techniques for calculating the forces and moments on aircraft surfaces caused by the propulsive efflux. Specifically, the type of jet/airframe interference problem explored is encountered with vectored engine exhausts. Although we will be discussing mainly the application to jet V/STOL aircraft, it is evident that the same prediction techniques are applicable to highly maneuverable aircraft employing vectoring-in-forward-flight, or aircraft employing in-flight thrust reversers.

An issue of major concern with jet-powered fixed wing V/STOL aircraft has been the lack of satisfactory methods for estimating the required lift thrust and control power from hover throughout transition to full wingborne flight. It is known widely that the propulsive jets induce a flowfield which can alter significantly the pressure distribution on the aircraft.[1] This effect can lead to forces and moments of the same order of magnitude as the conventional aerodynamic values, and is highly configuration dependent. Thus, to be a useful tool, it was necessary to evolve a three-dimensional prediction technique for complex multijet airframe configurations considering both in- and out-of-ground effects (OGE).

Inviscid wing/body panel methods and associated computer programs are available at government and industrial facilities.[2,3] These methods generally are adequate for preliminary design and development studies to describe the three-dimensional flowfield leading to aircraft forces and moments. Only a brief overview of the panel method will be presented here, since the theory and development of this calculation tool is detailed in the available literature.[2-4] The procedure evolved here extends this method, in that the aircraft, the multijets, and the ground plane all are subdivided into a large number of panels (Fig. 1), each containing a singularity (source/vortex) distribution. The usual zero normal velocity and Kutta condition for the aircraft surfaces are used, whereas the jets and ground plane wall jet region are treated as permeable surfaces through which mass influx is permitted. The prescription of the proper boundary condition on these latter surfaces is contingent upon accurate data, empirical or otherwise, describing the turbulent mixing process which causes entrainment of freestream air into the jet boundary.

The distinctive features relating to in-ground effects (IGE) will be described. During IGE a complicated flowfield is developed consisting of the formation of inclined wall jets interacting to form ground stagnation lines and fountains (Fig. 2). Because of deficiencies in the current knowledge of fountains (or upwash regions), the fountain region is not included in the panel method. Instead, simple momentum models are formulated which provide the ground stagnation lines, fountain location, inclination and strength, and conversion of fountain momentum into aircraft lift.

Finally, results of the prediction techniques will be shown for several cases where model test data are available. These include: a simplified aircraft configuration (OGE) in which the jet exit location relative to the wing was varied; a complicated six jet V/STOL fighter with various forward speeds; and supercirculation effects induced by vectoring a partial-span rectangular jet.

Theoretical and Numerical Potential Flow Solutions

The assumption of potential flow provides a useful tool for estimating the pressure distribution on bodies immersed in a steady external fluid. As long as the freestream total pressure losses are not large (because of wake regions and wall shear stresses), the solution of the Laplace equation (for subsonic flow) should provide an accurate first-order approximation.

Presented as Paper 75-1216 at the AIAA/SAE 11th Propulsion Conference, Anaheim, Calif., Sept. 29-Oct. 1, 1975; submitted Nov. 10, 1975; revision received March 17, 1976. The authors are grateful to J. Barche and his staff at VFW-Fokker, Bremen, Federal Republic of Germany, for providing an outstanding contribution by explaining and evolving the various theoretical and empirical elements required to form a comprehensive prediction technique. Portions of Barche's work are included in this paper. Gratitude is also extended to the Grumman Research Department, particularly to W. Hill, who provided the experimental results of multijets. Sponsored by Naval Air Propulsion Test Center (Exploratory Development Division) under Contract Number N00140-74-C-0113.

Index categories: Aircraft Aerodynamics (including Component Aerodynamics); VTOL Powerplant Design and Installation.

*Principal Investigator, Aerodynamics Section. Member AIAA.
†Project Engineer, Advanced Systems Technology. Member AIAA.
‡Research Scientist.
§Chief, Aerodynamics and Propulsion.
¶Program Manager for this study.

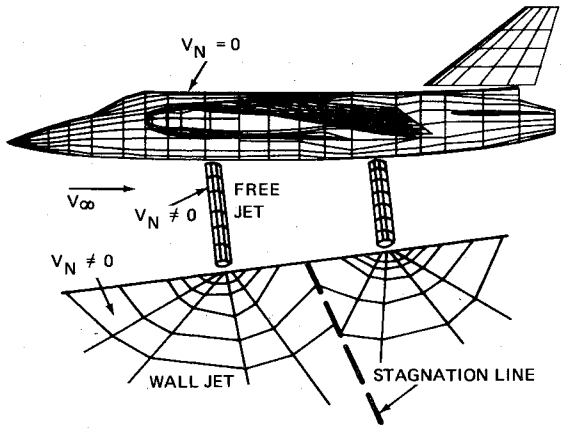

Fig. 1 Approach using panels with singularities.

In the so-called panel method of solution, the velocity potential is obtained by placing aerodynamic singularities on adjoining panels which simulate the body, and by prescribing the appropriate boundary conditions. For the Neumann problem, one of the boundary conditions is a specification of the gradient of the velocity potential normal to the body (i.e., the freestream velocity normal to the body). The jet flowfield also can be described with potential flow methods by selecting an appropriate surface and normal velocity.[5,6] Various wing/body and jet panel methods are described in the available literature.[2-6] The differences are mainly in the numerical procedure and selection of aerodynamic singularities (source, vortex, doublet, etc.).

We have been using two panel methods which are described briefly in the following. The first, which we call the OGE program, is presently a highly developed computerized tool and does not include IGE phenomena. The second, which we will call the IGE program, includes both in- and out-of-ground effects but requires increased computer time.

The OGE program is a Grumman wing/body panel technique for calculating the three-dimensional potential flow over complex configurations.[7,8] This program uses the source and vortex singularities developed in Refs. 2 and 4 for the aircraft and the Wooler sink-doublet model for the jet flowfield.[6] The sources on the aircraft panels (simulating body thickness) are assumed to be unchanged and the jet-induced effects are calculated by using only the vortex panel model of the aircraft. The vortex system is solved using a matrix inversion technique and aerodynamic coefficients which are saved on tape. Each jet on calculation provides a new set of airframe boundary conditions which is solved using the aerodynamic coefficients, yielding a modified vortex strength solution.

Theoretical Jet Models Out-of-Ground Effect

In the analytical model developed by Wooler, the sink-doublet singularities satisfy the three-dimensional Laplace equation and simulate both blockage and entrainment of freestream air. The theoretical analysis and empirical data used to simulate the freejet deformation and mass entrainment are developed thoroughly in Ref. 6. Snell[5] employs a panel method for the jets, where sinks are placed on a varying jet boundary to simulate blockage and entrainment. As opposed to the zero normal velocity condition for aircraft surfaces, a nonzero normal velocity boundary condition is imposed to simulate the mass entrained by the jet. In both approaches the jet shape, or surface, in a crossflow must be prescribed, adding further complications in unknowns that must be defined by empirical data.

By comparison with the foregoing, the freejet model adapted in the IGE program is considerably simplified. A reference jet boundary, identical to the jet exit cross section, is used for placing the sink distribution simulating mass entrainment. The entrainment factor (E) is thus simply

$$E = [d(\dot{m}/\dot{m}_J)]/[d(Z/R)] = -2(\rho_\infty V_n/\rho_J V_J)$$

where $\dot{m}$ is the mass flow, Z the curvilinear distance along the deflected jet, R the hydraulic radius of the jet, ρ the density (subscript J referring to jet, ∞ to freestream), V_J the jet velocity, and V_n the unknown normal velocity required at each panel along the jet. For circular jets, the normal inflow velocity V_n varies almost linearly from 2.5 to 8% of V_J from the initial region to fully developed flow, respectively. The inflow velocity remains constant at about 8%, starting at about six diameters downstream of the nozzle exit. The value of V_n can, of course, be adjusted depending on nozzle shape, temperature, Mach number, freestream velocity, and inclination. However, the empirical or theoretical data base to make such an adjustment still is limited severely.

It should be noted that, once the velocity potential is found for a given jet boundary and normal inflow velocity, the solution to Laplace's equation is unique and, thus, equivalent to any other singularity representation of the flow (such as vortices, sinks, doublets, etc.). A complete description of the many other facets of this problem would require more space than available in a paper of this nature. Reference 9 contains the semiempirical methods used to treat the entrainment of freejets in a crossflow, jet centerline deflection in a crossflow, and multijet interactions (OGE).

Theoretical Jet Models In-Ground-Effect

As shown in Figs. 1 and 2, in order to complete the potential flow theory for jet-induced effects, the wall jet region must also be modeled for IGE calculations. Our procedure involves dividing the ground plane into panels surrounding each jet impingement point. Singularities (sinks) are positioned on these panels. Since this type of modeling has not been presented previously, some additional details will be provided.

The singularities are positioned in the plane $z=0$, and the potential of a rotationally symmetric source distribution thus is given as

$$\phi(z,r,\varphi) = -\frac{1}{4\pi}\int_0^{2\pi}\int_R^\infty q(r',\varphi')\frac{r'\,dr'\,d\varphi}{r^*}$$

Here, r denotes the distance between a point $P(z,r,\theta)$ in the flowfield (Fig. 3) and a point $P'(o,r',\theta')$ on the wall, i.e.,

$$r^{*2} = z^2 + r^2 + r'^2 - 2rr'\cos(\varphi' - \varphi)$$

It is assumed that the inflow velocity of a wall jet decays hyperbolically with the radial distance r, but does not depend primarily on the circumferential angle φ. Since the source density q should be proportional to the entrainment, the potential ϕ can be a function only of z and r. Hence, the foregoing equations can be solved for any angle φ. The source strength q is not known but can be calculated by taking the Z derivative of ϕ and equating the resulting equation to the normal velocity simulating mass entrainment. This results in an integral equation for the unknown source strength.

Typical results for the induced velocity V_Z for an unbounded circular jet directed normal to the ground[9] are shown in Fig. 3. The rapid decay with height above ground and radial distance should be noted. For multijet configurations, the wall jet is bounded by stagnation lines where the flow is redirected because of interactions with other wall jets. Thus, a knowledge of interacting wall jets and the resulting flowfield is required. This is discussed in the following sections.

Multijet Interactions with a Ground Plane

The various flow regions and nomenclature are depicted in Fig. 4 for free jet ground impingement. For multijet configurations, interactions along the ground plane lead to

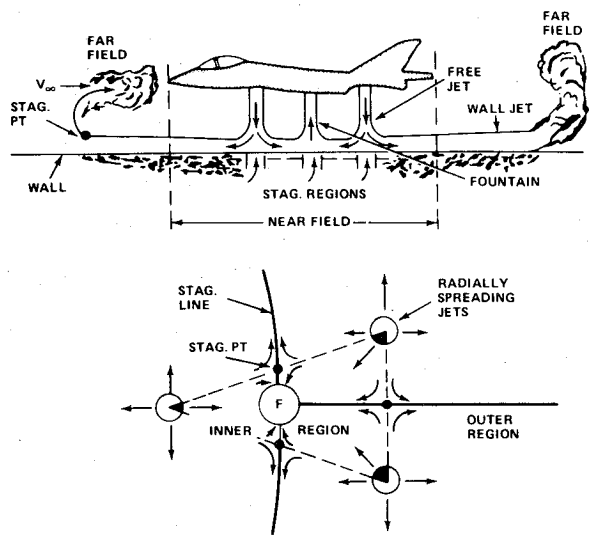

Fig. 2 VTOL aircraft flowfields.

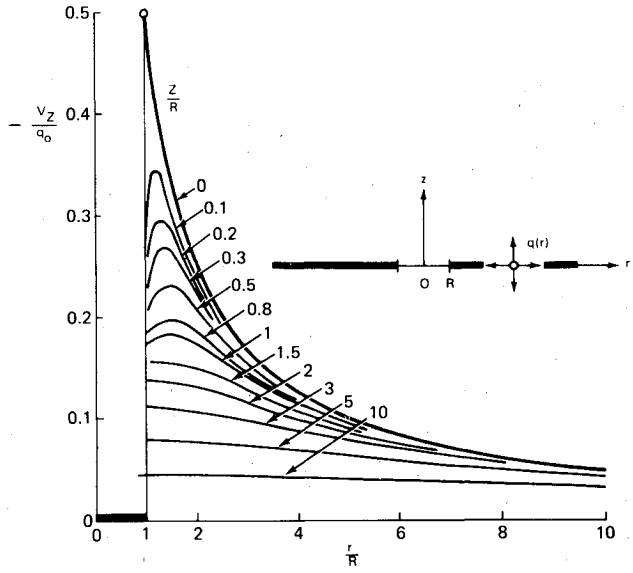

Fig. 3 Induced velocity for wall jet.

stagnation lines or dividing streamlines which can, in turn, produce upwash or distinct fountains as illustrated in Fig. 2. In treating the wall jet region the following assumptions were made:

1)The velocity profiles are similar, i.e.

$$C_n = \int_0^1 \left(\frac{V_r}{V_{r,m}}\right)^n d\left(\frac{Z}{h}\right) = \text{constant}$$

2) The gradient of the wall jet boundary h_r is constant and independent of the circumferential angle φ.

3) The wall jet origin is shifted from the impingement point as a function of nozzle swivel angle σ_j (defined by the parameter δ).

4) The initial height of the wall jet region h_0 is related to φ as follows:

$$h_0 = \bar{h}_0 + \Delta h \cos\varphi$$

5) The initial radial velocity V_{m0} is constant.

6) The wall jet maximum velocity decays as $1/r$.

7)Total pressure losses are neglected in the impingement and near-field region.

Some of the assumptions listed serve as starting points only, and can be modified easily in refined calculations. For example, experimental data can be used to correct for burning losses and wall shear forces. Other assumptions are based on a review of available wall jet data. For example, similar profiles are a commonly accepted description of the wall jet region, and the near hyperbolic decay of the maximum wall jet velocity also has been demonstrated experimentally.[10]

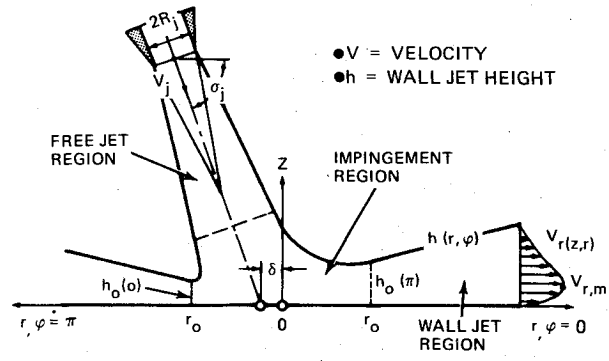

Fig. 4 Flow region leading to wall jet.

Wall Jet Momentum and Entrainment Velocity

In the wall jet region, a large amount of ambient air is entrained relative to the freejet region. With the assumptions just listed, two key phenomena can be estimated, namely, the mass entrainment and momentum decay per unit radial distance per unit circumferential angle φ.

The total momentum M of the freejet is assumed to be conserved and equal to the value at the nozzle exit M_J. In addition, neglecting shear forces, the integrated radial momentum also is constant and equal in magnitude to the value at the nozzle exit. With these assumptions, it can be shown that the wall jet momentum varies with r and φ as follows

$$\frac{\partial(\dot{M}/\dot{M}_j)}{r\partial\varphi} = \frac{1}{2\pi r}\left(1 + \frac{\Delta h}{h_r}\frac{\cos\varphi}{r}\right) \tag{1}$$

An expression for the radial mass flow in the wall jet can be developed in a manner similar to the development of the momentum flux. The mass flux at any radial position in the wall jet can be expressed as

$$\frac{\partial(\dot{M}/\dot{M}_j)}{r\partial\varphi} = \frac{c_i}{\pi R_j}\left(\frac{h_r}{2c_2}\right)^{1/2}\left(1 + \frac{\Delta h}{h_r r}\cos\varphi\right) \tag{2}$$

If a normal velocity is defined at the boundary of the wall jet, then the mass flux entrained through an incremental surface area is defined by

$$d\dot{m} = -2\rho V_n \pi r [1 + h_r^2]^{1/2} dr \tag{3}$$

Nondimensionalizing and taking the derivative with respect to φ leads to

$$[\partial(\dot{m}/\dot{m}_j)]/\partial r\partial\varphi = -[V_n r(1+h_r^2)^{1/2}]/V_j \pi R_j^2 \tag{4}$$

The normal velocity, required for entrainment calculations, is obtained by combining Eqs. (2) and (4) and assuming $h_r << 1$. The result is

$$-(V_n/V_j) \approx c_1 (h_r/2c_2)^{1/2}(R_j/r)$$

The open parameters h_r, C_1, C_2, Δh, and δ come from empirical data.

Stagnation or Dividing Streamline Theory

The equations established in the previous sections can be used for single jet effects. Most V/STOL aircraft, however, have more than one jet. For a multijet system each freejet may

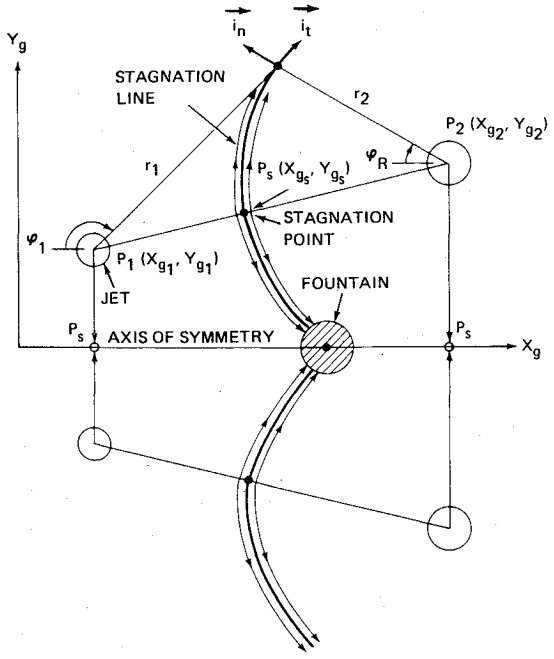

Fig. 5 Schematic of ground interaction region.

develop its own wall jet. As shown in Fig. 2, the individual wall jets are separated from each other by so-called "stagnation lines." A stagnation line is defined as that dividing line on which the stagnation point is located and where the condition of coflow exists in the two-dimensional ground plane system.

In order to predict jet-induced loads on an airframe, a simple approach was taken for which the following assumptions are made:

1) The flowfield is divided into an inner and outer region (see Fig. 2). In the inner region, all local momentum contributions concentrate into a fountain. In the outer region, all local momentum contributions are coflowing along the stagnation lines.

2) The stagnation lines, to a first order, are determined from the local momentum of a corresponding pair of jets; the contribution of other jets is assumed to be small.

With these assumptions, equations can be established that are applicable to either the inner or outer region for a pair of jets. Any multijet configuration can be formulated from these equations by superposition, and knowledge of the axes of symmetry.

For the nth jet, the basic equation (1) for the momentum flux in the radial direction is used. Each ground wall jet originates from the coordinates x_{g_n}, y_{g_n}, and has a momentum flux defined vectorally as $\boldsymbol{M}_{F_n} \equiv |\boldsymbol{M}_{F_n}| \boldsymbol{i}_{r_n}$, where

$$|\boldsymbol{M}_{F_n}| \equiv \frac{\partial \dot{M}_n}{r_n \partial \varphi_n} = \frac{\dot{M}_{jn}}{2\pi r_n}\left[1 + \frac{\Delta h_n}{h_{r_n}}\frac{\cos\varphi_n}{r_n}\right]$$

As illustrated in Fig. 5, the direction of the dividing line is defined, a priori, by a unit tangential vector $\boldsymbol{i}_T$ whose inclination makes an angle with the positive streamline direction and whose unit normal vector is $\boldsymbol{i}_N$. In the ground fixed coordinate system, these vectors are defined as

$$\boldsymbol{i}_N = \boldsymbol{i}_{y_g}\cos\theta - \boldsymbol{i}_{x_g}\sin\theta$$

$$\boldsymbol{i}_T = \boldsymbol{i}_{x_g}\cos\theta + \boldsymbol{i}_{y_g}\sin\theta$$

If a nondimensional jet-centered coordinate system is introduced, i.e.

$$\xi_n \equiv (x_g - x_{g_n})/\ell,\ \eta_n \equiv (y_g - y_{g_n})/\ell$$

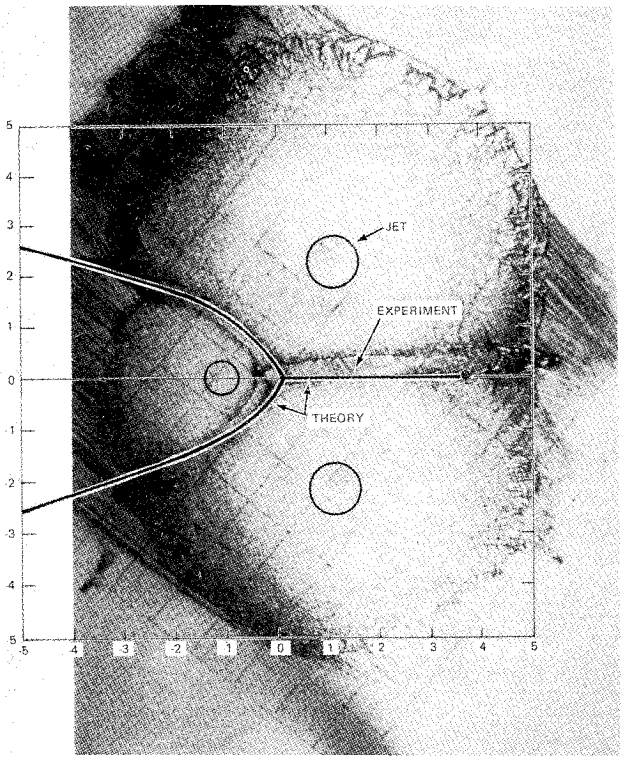

Fig. 6 Three-jet group with central fountain.

then

$$r_n^* \equiv r_n/\ell = (\xi_n^2 + \eta_n^2)^{1/2}$$

The unit radial vector of a jet can be defined in this ground system as

$$\boldsymbol{i}_{r_n} = (\xi_n \boldsymbol{i}_{x_g} + \eta_n \boldsymbol{i}_{y_g})/r_n^*$$

At any point on the stagnation line the coflow condition must exist, or

$$\sum_1^n [\boldsymbol{M}_{F_n} \cdot \boldsymbol{i}_N] = 0$$

which implicitly defines the inclination of the stagnation line. Solving for the slope, this equation becomes, for a pair of jets

$$\tan\theta = \frac{\eta_1 r_2^{*2}\left(1 - \frac{\lambda_1\xi_1}{r_1^{*2}}\right) + m\eta_2 r_1^{*2}\left(1 - \frac{\lambda_2\xi_2}{r_2^{*2}}\right)}{\xi_1 r_2^{*2}\left(1 - \frac{\lambda_1\xi_1}{r_1^{*2}}\right) + m\xi_2 r_1^{*2}\left(1 - \frac{\lambda_2\xi_2}{r_2^{*2}}\right)} \tag{5}$$

where

$$m \equiv \dot{M}_{j2}/\dot{M}_{j1} \text{ and } \lambda_n = \Delta h_n/\ell(h_r)_n$$

The solution of Eq. (5) was obtained using a step-by-step numerical iterative procedure. The stagnation points (Fig. 2) are calculated first, and the stagnation lines are constructed proceeding (numerically) in the direction of the inner and outer regions. Fountain origin(s) are defined as the intersection of the stagnation lines with the axis of symmetry (i.e., the aircraft centerline in plane view).

Despite the simplified theoretical approach just outlined, the results are quite representative of the actual flow phenomena. Ground flow oil visualization studies were performed by the Grumman Research Department. The

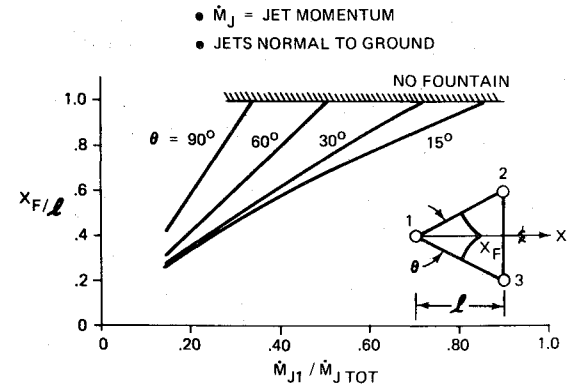

Fig. 7 Fountain origin for three-jet groups.

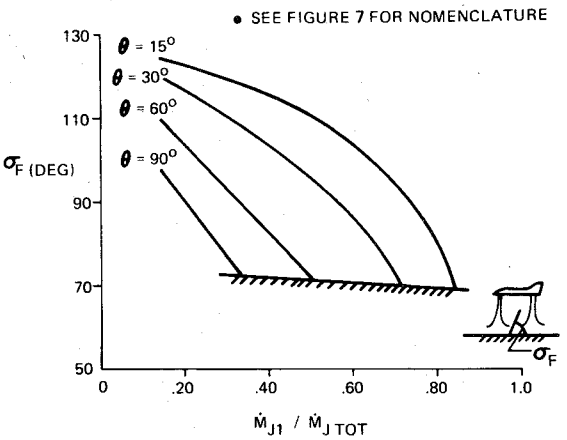

Fig. 8 Fountain inclination for three jet groups.

theoretical stagnation lines are compared to these experimental data in Fig. 6 for a three-jet group with differing momentum ratios. In Fig. 6, with one small jet on the axis of symmetry, a single fountain is observed near the small jet. Note also that the stagnation lines wrap around the lower strength centerline jet, and that the agreement between theory and experiment is quite good. Depending on the strength and number of the various jets, multifountain regions can occur, or the strong central fountain can be eliminated.

Fountain Properties

Having defined the fountain region from the stagnation line theory, the additional properties of interest are the fountain origin location, the inclination of the fountain as it leaves the ground, and the fountain momentum. If the predicted origin lies outside the inner region, then, in fact, there is no strong central fountain. Parametric theoretical results for a three-jet group, with various spacing ratios and jet strengths, are shown in Fig. 7. For values of the abscissa greater than one, the stagnation lines intersect the axis of symmetry outside the inner region, thus indicating no central fountain.

When there is a strong central fountain, the fountain inclination relative to the ground plane (Fig. 8) determines which portion of the aircraft will experience the highest temperatures and pressures. The fountain inclination is obtained by integrating Eq. (1) to obtain the net X value (Fig. 5) of momentum in the inner region for all jets. The net X value of momentum at the fountain origin divided by the total momentum in the inner region is the cosine of the fountain inclination angle. Generalized theoretical results for a three-jet grouping are shown in Fig. 8. These results were obtained for vertical jets and reveal a wide variation in fountain inclination, depending on jet spacing and strength. Such information is very useful in the preliminary design and test phases to determine the potential problem areas and, ultimately, inlet reingestion temperature rise.

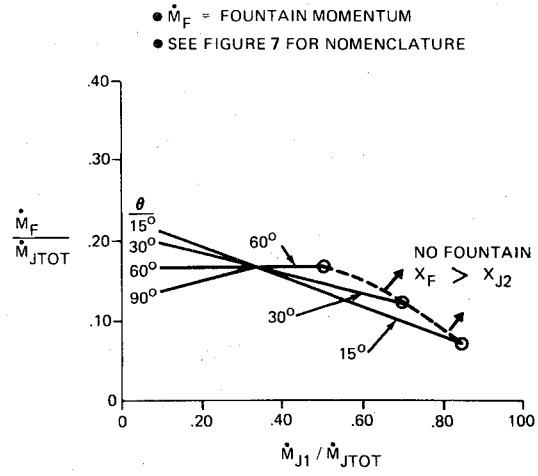

Fig. 9 Fountain strength for three-jet groups.

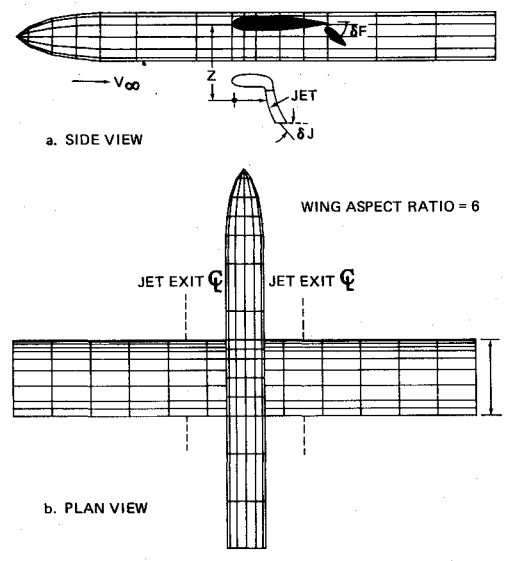

Fig. 10 Panel representation of NASA test model.

Again, when there is a central fountain, the total momentum is obtained by integrating Eq. 1 for the inner region only. Parametric results, for the same variables and conditions shown in Figs. 7 and 8, are depicted in Fig. 9. Here the fountain momentum is shown as a fraction of the total jet momentum. These theoretical results indicate that 10% to 20% of the total jet thrust is available for conversion to fountain lift on the aircraft. Other features of the theory that are noteworthy are: the value of fountain momentum is insensitive to jet strength when the resulting tri-jet group results in an equilateral triangle; and, increasing jet spacing (i.e., increasing values of θ, Fig. 9) increases the fountain momentum only when the centerline jet momentum (jet 1) is greater than 0.33 of the total momentum.

Knowledge of the foregoing fountain properties (i.e., location, inclination, and momentum) is required to calculate the conversion of fountain momentum into aircraft lift. This calculation is configuration sensitive, in that the aircraft geometry at the fountain impingement point will determine the net lift. No generalized data base is available at this time for predicting the fountain conversion factors, and each case must be examined in detail to approximate the fountain lift.

Results

Some generalized results for the IGE program were presented in the previous section. This method, although quite versatile and useful (especially for IGE phenomena) requires a large number of panels and the solution of a large system of

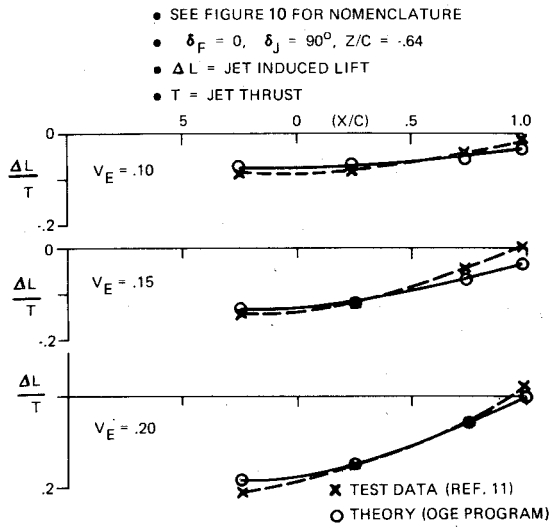

Fig. 11 Variation of jet-induced lift with longitudinal jet location.

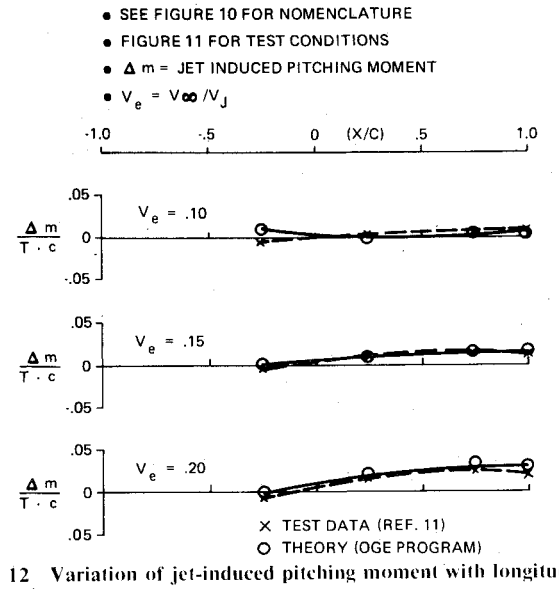

Fig. 12 Variation of jet-induced pitching moment with longitudinal jet location.

simultaneous linear equations. The source and vortex system is solved simultaneously by a numerical iterative procedure and must be performed for each jet on calculation. In contrast, the Grumman OGE program runs quite rapidly and can handle a large number of cases for which experimental data are available. In this section we will present correlatons obtained with this program for out-of-ground conditions.

Simple Twin Jet V/STOL Configuration

In 1969, NASA experimental data were reported in which the effects of jet exhaust location were investigated for a simplified twin-jet V/STOL model.[11] The center body was cylindrical, the wing planform rectangular, and each jet was located a quarter semispan outboard of the model centerline with both vertical and longitudinal translation capability. Since the jets were mounted separately, only jet-induced forces were measured on the aircraft balance.[11]

Because of the simple geometry of this model, the vortex panel model closely resembles the source model for this configuration, and is shown in Fig. 10. A vertical jet located 0.64 of the chord below the wing was chosen for performing the theoretical calculations to minimize experimental jet wake effects (which are not accounted for in the potential flow modeling). The test data and theoretical results are compared in Fig. 11 for jet-induced lift and in Fig. 12 for jet-induced

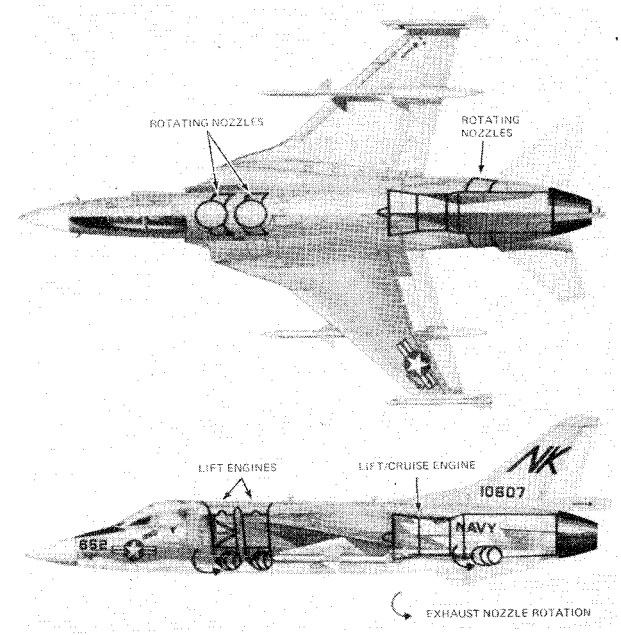

Fig. 13 Schematic of supersonic V/STOL aircraft.

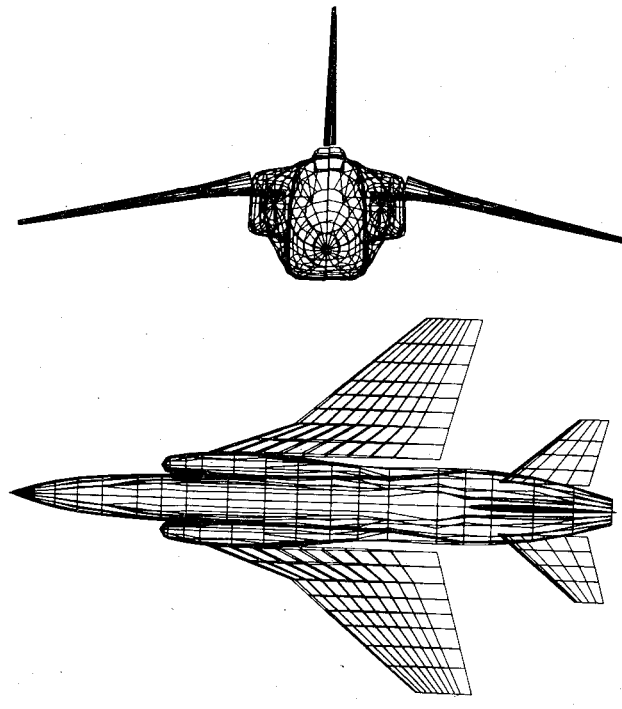

Fig. 14 Panel representation of jet V/STOL aircraft.

pitching moment. The effects of jet exit axial location (X/C) and velocity ratio (freestream/jet exhaust) are predicted remarkably well, although an entrainment parameter adjustment was necessary to achieve the correlation shown.

Six Jet V/STOL Fighter Configuration

A ⅛th-scale model (Fig. 13) of an aircraft with two forward mounted lift engines and a fuselage mounted lift cruise engine was tested by Grumman in the British Aircraft Corporation 5.5m-V/STOL-tunnel. Each engine had a pair of nozzles, thus, a total of six jet exhausts. The panel representation of this model is shown in the two views of Fig. 14.

The jet-induced lift and moment characteristics for typical nozzle deflection angles are shown in Fig. 15. The jet-induced lift loss predictions show excellent correlation with test data over a range of nozzle deflection angles and velocity ratios.

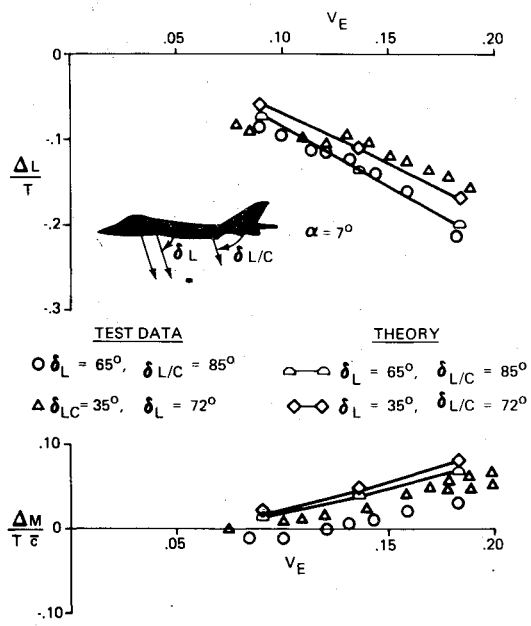

Fig. 15 Predicted and experimental jet-induced characteristics.

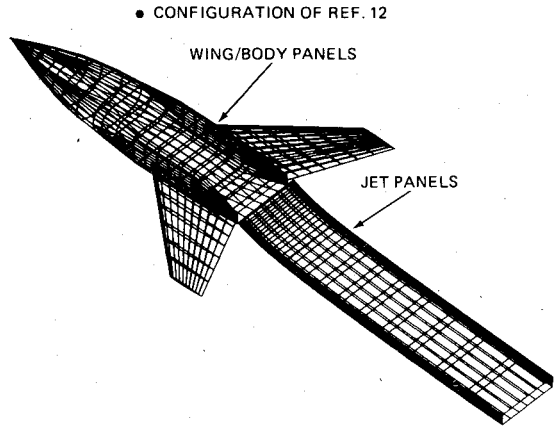

Fig. 16 Panel representation of NASA supercirculation test model.

The predicted induced moment compared fairly well in slope but exhibits slightly higher magnitude than the test data.

Supercirculation Effects Caused by Jet Vectoring

Recent experimental studies reported by Capone of NASA-Langley indicated the possibility of increases in lift due to thrust vectoring with the jets located at the wing trailing edge. Details of the model setup and test results are contained in Ref. 12. The Grumman OGE program was utilized in order to determine if the measured supercirculation effects are, in fact, predictable. The panel model of the simulated aircraft and rectangular jet exhaust is shown in Fig. 16. The rectangular nozzle, for the OGE method, was simulated using four closely-spaced circular jets with the same total thrust.

The power-induced effects for a typical jet deflection angle of 30° are shown in Fig. 17. Even using the rather simplified approach (four circular nozzles to simulate one rectangular nozzle), very good agreement between the theoretical and test results was obtained.

Conclusion

Several theoretical approaches for predicting the jet-induced effects on aircraft forces and moments have been presented for both in- and out-of-ground effects. The resulting prediction technique requires an extensive computer program, but is applicable to truly three-dimensional flows and is the most comprehensive V/STOL jet-induced method presented to date. Some excellent correlations for OGE and

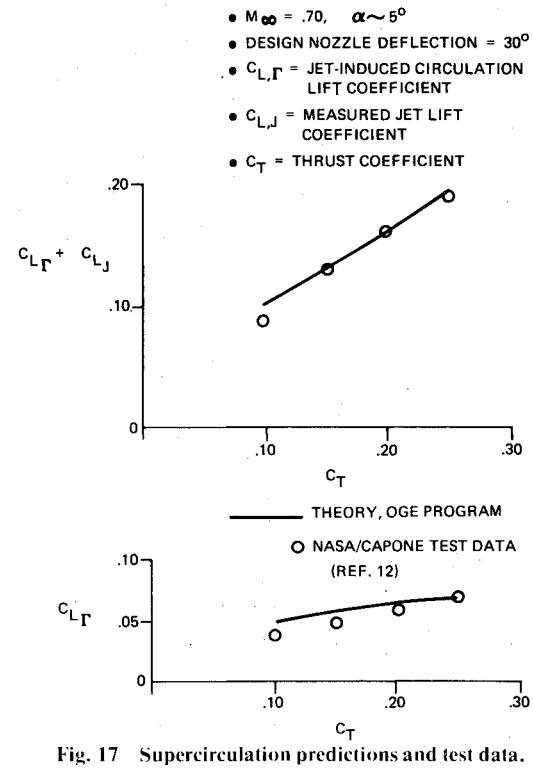

Fig. 17 Supercirculation predictions and test data.

portions of the IGE flow were shown. One of the key areas for improving the prediction technique concerns the entrainment characteristics of single and multijets (in- and out-of-ground effect) with and without crossflows, and the effect of nozzle shape and thermodynamic properties on entrainment. Another area where basic data are severely limited is the fountain flow or upwash region.

References

[1]Margason, R.J., "Review of Propulsion-Induced Effects on Aerodynamics of Jet V/STOL Aircraft," N70-18243, Feb. 1970, U.S. Dept. of Commerce, NTIS.

[2]Woodward, F.A., "A Computer Program for the Analysis and Design of Wing-Body-Tail Combinations at Subsonic and Supersonic Speeds," TN-12, May 1968, Aerophysics Research Corp.

[3]Woodward, F.A. "An Improved Method for the Aerodynamic Analysis of Wing-Body-Tail Configurations in Subsonic and Supersonic Flow," CR-2228, May 1973, NASA.

[4]Hess, J.L. and Smith, A.M.O., "Calculations of Potential Flow About Arbitrary Three-Dimensional Bodies," Rept. E.S. 40622, 1962, Douglas Aircraft Corp.

[5]Snel, H. "A Method For The Calculation of Flow Field Induced By A Jet Exhausting Perpendicularly Into A Crossflow," CP-143, April 1974, AGARD, Delft, Netherlands.

[6]Wooler, P.T., Kao, H.C., Schwendemann, M.F., Wasson, H.R. and Ziegler, H., "V/STOL Aircraft Aerodynamic Prediction Methods Investigation," TR-72-26, Jan. 1972, Air Force Flight Dynamics Laboratory.

[7]Boppe, C.W., "A Computer Program for Calculating the Subsonic Aerodynamics of Complex Wing-Body Configurations," Rept. 393-73-1, 1973, Grumman Aerospace Corp.

[8]Siclari, M.J., "Subsonic Aerodynamic Prediction Method for Jet Induced Effects on Complex Wing-Body Configurations," ADR, June 1975, Grumman Aerospace Corp.

[9]Siclari, M.J., Barche, J., and Migdal, D., "V/STOL Aircraft Prediction Technique Development For Jet Induced Effects," PDR 623-18, April 1975, Grumman Aerospace Corp.

[10]Gaunter, J.W., "Survey of Literature On Flow Characteristics of a Single Turbulent Jet Impinging on a Flat Plate," TN-D-5652, Feb. 1970, NASA.

[11]Carter, A.W., "Effects of Jet-Exhaust Location on the Longitudinal Aerodynamic Characteristics of a Jet V/STOL Model," TN D-53333, July 1969, NASA.

[12]Capone, F.J., "Supercirculation Effects Induced By Vectoring a Partial-Span Rectangular Jet," AIAA Paper 74-971, Los Angeles, Calif., Aug. 1974.